Universal Journal of Catalysis Science
https://ojs.wiserpub.com/index.php/UJCS/

Research Article

Study of Gas-phase Reactions within the Modified Marcus Model. V. Arrhenius Equation for the Reaction $CH_3OH + CH_3 \rightarrow CH_2OH + CH_4$

Igor Romanskii

Institut himiceskoj fiziki imeni N N Semenova RAN Moscow, Russian Federation
Email: ceng37@yandex.ru

Received: 4 April 2023; **Revised:** 14 August 2023; **Accepted:** 6 September 2023

Abstract. A theoretical study of the kinetics of the gas-phase reaction $CH_3OH + CH_3 \rightarrow CH_2OH + CH_4$ (energy calculation level UCCSD (T)/6-311G**//B3LYP/6-31+G**) in the temperature range 2000–10 K was performed. A discussion is carried out within the framework of a modified version of the Marcus model. The obtained results are used to analyze the Arrhenius equation in terms of the change in temperature of each of the parameters included in the expression for the reaction rate constant. In accordance with the change in the influence of various factors on the shape (slope and curvature) of the Arrhenius plot, the temperature intervals 2000 - 600, 600 - 80 and 80 - 10 K are distinguished.

Keywords: Methanol, methyl radical, hydrogen atom transfer, non-equilibrium model, Arrhenius equation

1. Introduction

This work continues the earlier study of methanol with methyl radical gas-phase reaction kinetics [1] (Eq. 1) in the framework of a modified version of the non-equilibrium Marcus model [2, 3]. The study, compared to the previous, includes two changes: (1) the range of temperatures has been extended from 550 -10 K to 2000 - 10 K and (2) the UCCSD (T)/6-31+G** energy calculation level has been replaced by UCCSD (T)/6-311G** (at the geometry optimization, the B3LYP/6-31+G** basis was retained).

$$CH_3OH + CH_3 \rightarrow CH_2OH + CH_4 \quad (1)$$

The main purpose of the work is to analyze the Arrhenius equation. As in the work on the reaction of methane with a methyl radical [4], the discussion developed in terms of changes in temperature of each of the parameters included in the reaction rate constant equation. In accordance with the nature of the influence of various parameters on the form of the Arrhenius plot, the temperature ranges of 2000 - 600, 600 - 80 and 80 - 10 K are distinguished.

2. Theoretical model

The theoretical models of the proton and hydrogen atom reaction in the solution approach [2,3,5,6] are based on the generalized Frank-Condon principle (GFCP) [7], according to which during the proton tunneling the heavy

DOI: https://doi.org/10.37256/ ujcs.1220232782

atoms of the system retain their positions. The adequate GFCP (somewhat simplified) scheme of the hydrogen atom (hereafter H-atom) transfer reaction includes the following stages:

(1) approach of the reactants to a certain distance Q between the H-atom donor and acceptor atoms;

(2) non-equilibrium (H atom in the initial state) reorganization of the system: movement of the system along the structural coordinate q at a fixed distance Q;

(3) tunneling of hydrogen: the movement of the H atom along its coordinate r at fixed parameters Q and q;

(4) relaxation of reaction products and their separation.

For a fixed distance Q, the potential of the system along the H-atom coordinate r, $V(r|Q)$, is double-well. The stage of reorganization consists of potential $V(r|Q)$ symmetrization. The symmetrization requirement follows from the energy conservation law in the form of the need to equalize the vibrational levels of the H-atom in the potential left and right wells.

In [1], this approach was applied to proton (and hydrogen atom) transfer reactions in the gas phase. The most significant change in the proposed model concerned the structural coordinate of the reaction. Instead of the multidimensional coordinate q, which in the case of a gas-phase reaction includes all the internal coordinates of the system, use of the one-dimensional proton coordinate r was proposed. In this regard, we considered a hypothetical situation corresponding to the equilibrium (at a fixed distance Q) motion of the system along the coordinate r. In order to distinguish this slow motion along r from the fast process of H-atom tunneling, the symbol ρ was assigned to the coordinate r in this case. The ρ coordinate is a new structural coordinate, since the movement along ρ, like the movement along the q coordinate, is accompanied by non-equilibrium reorganization of the system. Since in both cases we are talking about changing the same potential of the system, V, at a fixed distance Q, there is a one-to-one correspondence between the potentials $V(q|Q)$ and $V(\rho|Q)$. A similar correspondence also takes place between the coordinates q and ρ. The latter means that any point on the q coordinate can be associated with a certain point on the ρ coordinate, and vice versa. This, in fact, determines the possibility of replacing the multidimensional coordinate q with the one-dimensional coordinate ρ. The immediate advantage of such a replacement is the possibility of determining the geometry of the activated complex (AC) of the H-atom transfer reaction using the procedure of partial (at fixed values of the parameters Q and ρ) geometry optimization; this procedure is standard in software packages such as the Gaussian program. As a result, it becomes possible for ab initio calculation of the geometry (and energy) of a non-equilibrium AC in the general case of an asymmetric reaction.

Within this model, the thermal rate constant, $k(T)$, is calculated using the equation:

$$k(T) = \sigma \int \nu_t(Q,T)\, \exp[-\Delta G^*(Q)/RT]\, dQ \tag{2a}$$

$$\Delta G^*(Q) = \Delta H^*(Q) - T\Delta S^*(Q) \tag{2b}$$

$$\Delta H^*(Q) = E_a(Q) + \Delta h^*(Q) \tag{2c}$$

$$\Delta S^*(Q) = 1000\, \{[\Delta h^*(Q) - \Delta g^*(Q)]/T\} \tag{2d}$$

$$\Delta h^*(Q) = h^*(Q) - h;\ \Delta g^*(Q) = g^*(Q) - g \tag{2e}$$

where σ is the symmetry number (for Reaction (1) σ = 3); ν_t is the tunneling frequency in the symmetric potential $V(r|Q,\rho^*)$ (ρ^* - ρ coordinate for AC), ΔG^*, ΔH^* and ΔS^* are the free energy, enthalpy and entropy of activation, respectively, E_a is the electronic activation energy of the reaction, Δh^* and Δg^* are the thermal corrections to the enthalpy and the free activation energy, respectively, where $h^*(h)$ and $g^*(g)$ are the corresponding thermal corrections for the AC (reagents); and R is the gas constant. The calculation of thermodynamic parameters is performed in the rigid rotor approximation without accounting for free and internal rotations of the AC and reactants.

The energy E_a is defined as the sum of the equilibrium, E_a^{eq}, and nonequilibrium, E_a^{neq}, components[1]:

$$E_a = E_a^{eq} + E_a^{neq} \tag{3}$$

To calculate the tunneling frequency $\nu_t(Q,T)$ the following relation is used:

[1] In Marcus theory, the free-energy analogs of E_a^{eq} and E_a^{neq} energies are, respectively, the "working member" w_r and the free activation energy in the collision complex, ΔG^*.

$$\nu_t(Q,T) = \nu_t^{00}(Q) + \Sigma_i\, \nu_t^{i}\,(Q,T) \tag{4a}$$

$$\nu_t^{i}\,(Q,T) = \nu_t^{ii}(Q)\, exp(\Delta V_{i0}(Q)/RT) \tag{4b}$$

where ν_t^{00} and ν_t^{ii} are the frequencies of H-atom tunneling between zero levels and the i-th levels of the double-well potential $V(r|\rho^*,Q)$, respectively, and ΔVi_0 is the energy difference between the i-th and zero levels of the potential.

Due to the opposite changes with the distance Q of the frequency and exponential terms in Eq. 2a, the integrand passes through a maximum at some distance $Q = Q_m$. It was found that the calculation according to the equation for $k(T)$ at the point Q_m, $k_m(T)$ (Eq. 5), leads to the results, which are very close to the results of the calculation with Eq. 2 (see below).

$$k_m(T) = \sigma\, A_m\, exp(-\Delta H_m^*/RT); \tag{5a}$$

$$A_m = \nu_t^{m}\, exp(\Delta S_m^*/R); \tag{5b}$$

$$\Delta H_m = E_a^{m} + \Delta h_m^* \tag{5c}$$

According to Eq. 4 the frequency ν_t^m is defined as a cumulative quantity:

$$\nu_t^{m} = \nu_{t,m}^{\,0} + \nu_{t,m}^{\,i}\,, \tag{6a}$$

where

$$\nu_{t,m}^{\,0} = \nu_t^{00}(Q_m) \tag{6b}$$

and

$$\nu_{t,m}^{\,i} = \Sigma_i\, \nu_t^{i}\,(Q_m,T)\,. \tag{6c}$$

The description of the reaction rate constant k_m as a function of temperature presented below is based on a detailed analysis of Eqs.5 and 6.

3. Calculation details

The procedure for calculating the AC geometry and energy at a given distance Q, including partial optimization of the system geometry at fixed values of the Q and ρ^* distances and the $OC_1C_2H_4$ dihedral angle (180°, Scheme), was described earlier [1]. All calculations were performed using the GAUSSIAN 03 software package [10] at the UCCSD(T)/6-311G**//B3LYP/6-31+ G** level. Frequencies ν_t (Eqs. 4 and 6) are calculated in the WKB approximation by the Brikkman method [11,12].

Scheme

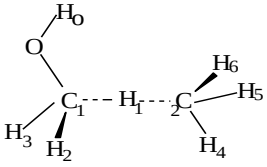

A distinctive feature of this model is the imaginary frequencies that appear in the calculation of the AC thermochemical functions h^* and g^*. In the present model, the complex is considered a quasi-stable formation, and the process of tunneling from the left to the right well of the potential $V(r|\rho^*,Q)$ is considered, relatively, a

transition from one stable non-equilibrium state to another similar state. For this reason, the presence of imaginary frequencies is considered an artifact associated with fixation in the calculation of several geometric parameters[2].

4. Results and discussion

4.1 *Energetics, frequencies*

In Table 1 the reaction energy, ΔE_{00}, and the saddle point barrier height, E_{SP}, calculated from these data, are compared with the corresponding data of [1] and the results of calculations by Truhlar et al. [14] obtained in the framework of the variational TST (multi-structural canonical variational transition-state theory with multidimensional tunneling (MS-CVT/MT)).

Table 1. Reaction energy, ΔE_{00}, and barrier height at saddle point, E_{SP} (kcal.mol^{-1})

Parameter	This work[a)]	[1][b)]	[14][c)]
ΔE_{00}	-9.2	-7.7	-9.01
E_{SP}	14.0	16.3	13.69

a) UCCSD(T)/6-311G**//B3LYP/6-31+G**; b) UCCSD(T)/6-31+G**//B3LYP/6-31+G**; c) CCSDT(2)/CBS// M06-2X/MG3S

As seen from the table, the transition in the energy calculation from the UCCSD(T)/6-31+G** basis [1] to UCCSD(T)/6-311 G** significantly improves agreement with the article [14] data.

The values of the energies E_a^{eq}, E_a^{neq}, E_a and E_b are given in Table 2. These data are illustrated in Figure 1, which shows the profiles at Q = 3.0 A with $\rho = r_{01}$ (a) and $\rho = \rho^*$ (b).

Table 2. Energies E_a^{eq}, E_a^{neq}, E_a, E_b (kcal.mol^{-1}) and coordinate ρ^* (Å) in the dependence from Q (Å).

Q	E_a^{eq}	E_a^{neq}	E_a	E_b	ρ^*	Q	E_a^{eq}	E_a^{neq}	E_a	E_b	ρ^*
2.6	14.93	0.01	14.94	1.00	1.107	3.3	1.37	1.40	2.77	29.12	1.433
2.7	11.49	0.11	11.60	3.55	1.149	3.4	0.75	1.66	2.41	33.69	1.483
2.8	8.72	0.28	9.00	6.93	1.193	3.5	0.29	1.98	2.27	38.12	1.531
2.9	6.47	0.51	6.98	10.86	1.240	3.6	-0.03	2.34	2.31	42.36	1.581
3.0	4.69	0.71	5.40	15.23	1.286	3.7	-0.25	2.74	2.49	46.40	1.629
3.1	3.28	0.92	4.20	19.81	1.322	3.8	-0.40	3.21	2.81	50.17	1.678
3.2	2.19	1.15	3.34	24.45	1.385						

[2] The appearance at these requirements of a negative frequency value may be due to a change in the shape of the oscillatory potential – from one- to double-well.

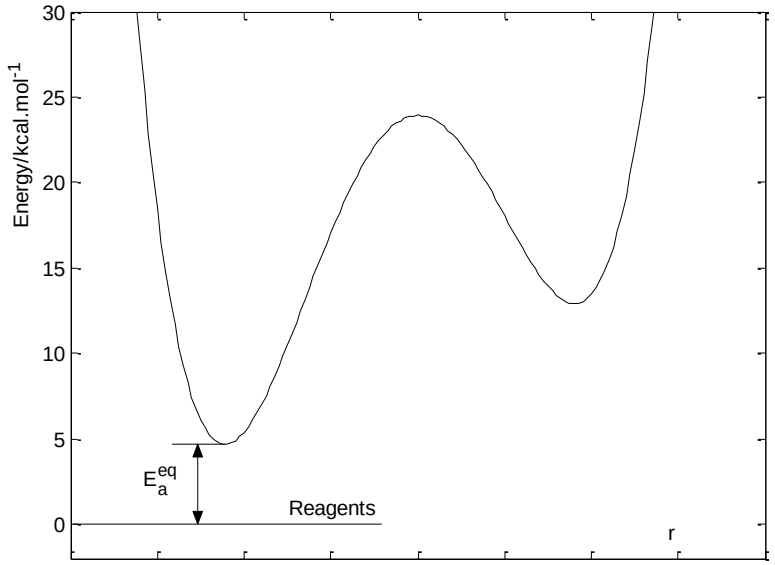

Figure 1a. The energy profile of the system along the coordinate *r* by the time of reagents approach, $V(r|\rho=r_{01},Q)$ at Q = 3.0 Å.

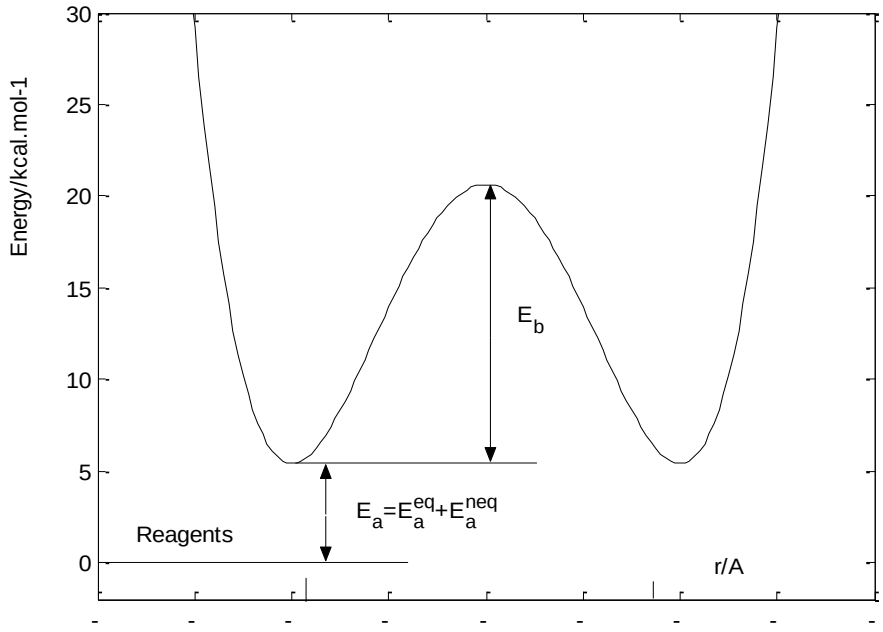

Figure 1b . The energy profile of the system along the coordinate *r* in the activated complex, $V(r|\rho=\rho^*,Q)$; Q = 3.0 Å, ρ^* = 1.286 Å.

Opposite, depending on Q, changes in energies E_a^{eq} and E_a^{neq} (Table 2) lead to the appearance of a minimum, E_a^{min} = 2.27 kcal.mol^{-1}, at Q_{min} = 3.5 A (Figure 2). A similar type of dependence $E_a(Q)$ is observed for the reaction of methane with a methyl radical [4].

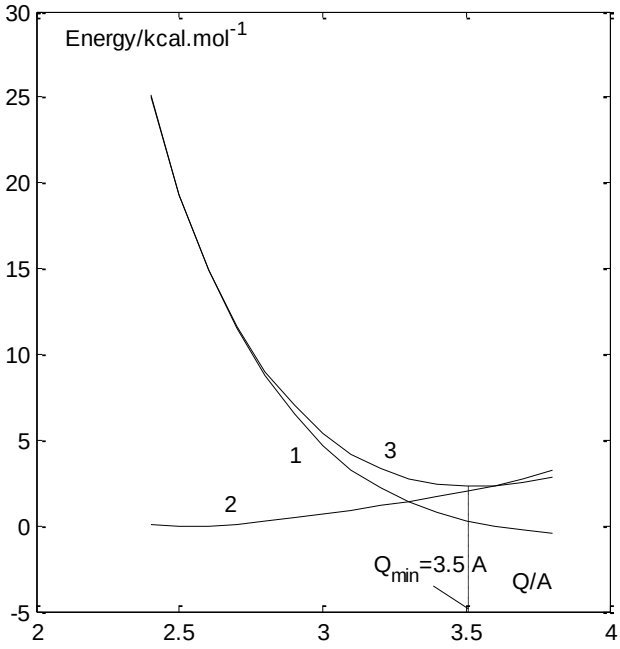

Figure 2. Dependence of the energies E_a^{eq} (curve 1), E_a^{neq} (curve 2) and E_a (curve 3) on the distance Q.

As noted (Section 3) the method adopted in this approach for calculating the thermo-chemical functions of AC (h^* and g^*) involves replacing imaginary frequencies with corresponding real values. At all temperatures, three imaginary frequencies are observed for AC, showing some dependence on the distance Q (Table 1S of the Supplementary Materials). The values of h^* and g^* calculated by the standard method are given, respectively, in Tables 2S and 3S and the corrected (taking into account imaginary frequencies) values of h^* and g^*, together with the values of h and g of the initial reagents are provided in Tables 4S and 5S.

4.2 *Rate constants*

The results of calculating the values of the rate constants k (Eq. 2) and k_m (Eq. 5) for temperatures 2000 - 10 K are given in Table 3 and Figures 3 and 4. A relatively small difference in the values of k_m and k reveals a weak temperature dependence: in the range from 2000 to 80 K, the k_m/k relation changes from 2.5 to ~ 5 and only at the lowest temperatures increases to 13-18. The reason for the change in the k_m/k relation is a decrease in the effective Q interval: from ~0.9 Å at 2000 K to ~0.5 Å at 80 K and to ~0.2 Å at 10 K.

Table 3. Rate constants k and k_m ($l.mol^{-1}.s^{-1}$)

T, K	k	k_m	T, K	k	k_m
2000	1.08(8)	2.60(8)	250	0.829	3.78
1800	5.82(7)	1.46(8)	200	0.0424	0.181
1500	1.75(7)	4.86(7)	150	5.32(-4)	2.77(-3)
1200	3.69(6)	1.18(7)	120	1.26(-5)	5.97(-5)
1000	8.93(5)	3.10(6)	100	4.31(-7)	2.33(-6)
800	1.42(5)	5.39(5)	80	4.41(-9)	2.14(-8)

600	1.01(4)	4.12(4)	60	3.53(-12)	2.18(-11)
550	3.61(3)	1.56(4)	40	5.86(-18)	4.51(-17)
500	1.62(3)	7.10(3)	30	1.59(-23)	1.39(-22)
450	606	2.56(3)	20	1.37(-34)	1.21(-33)
400	176	794	15	1.37(-45)	1.81(-44)
350	40.8	192	10	1.19(-67)	2.13(-66)
298.15	6.16	27.4			

In the range 2000 – 80 K (Figure 3), the temperature dependences of the constants k (curve 1) and k_m (curve 2) are well described by equations of the fourth degree (respectively, Eqs. 7 and 8); at 80 -10 K (Figure 4), both dependences are linear (Eqs. 9 and 10).

$$\log k = 5.32\ t^4 - 20.87\ t^3 + 31.12\ t^2 - 27.00\ t + 10.60 \quad (7)$$

$$\log k_m = 4.74\ t^4 - 18.36\ t^3 + 27.40\ t^2 - 24.77\ t + 10.79 \quad (8)$$

$$\log k = -3.10\ t + 0.26 \quad (9)$$

$$\log k_m = -3.07\ t + 0.94 \quad (10)$$

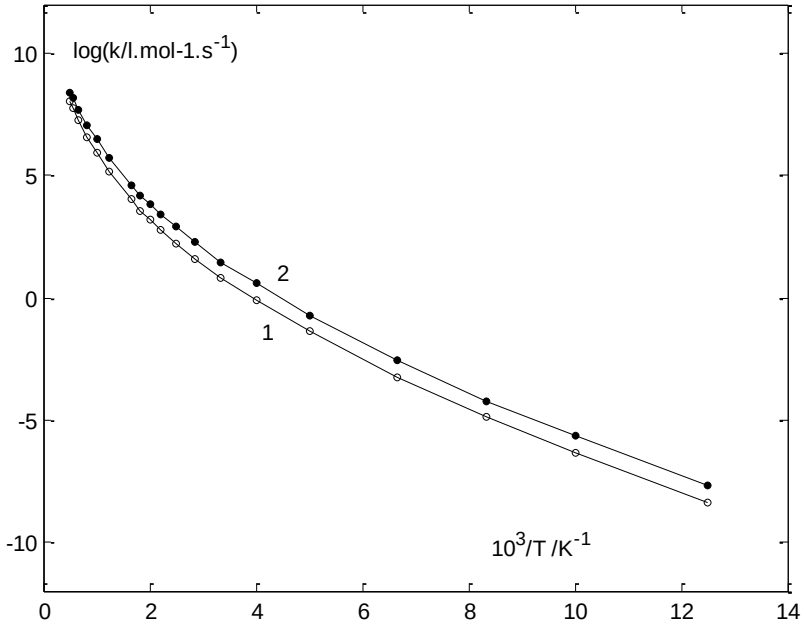

Figure 3. The rate constants k over the interval 2000 – 80 K: 1 k (Eq. (3)), 2 k_m (Eq. (6))

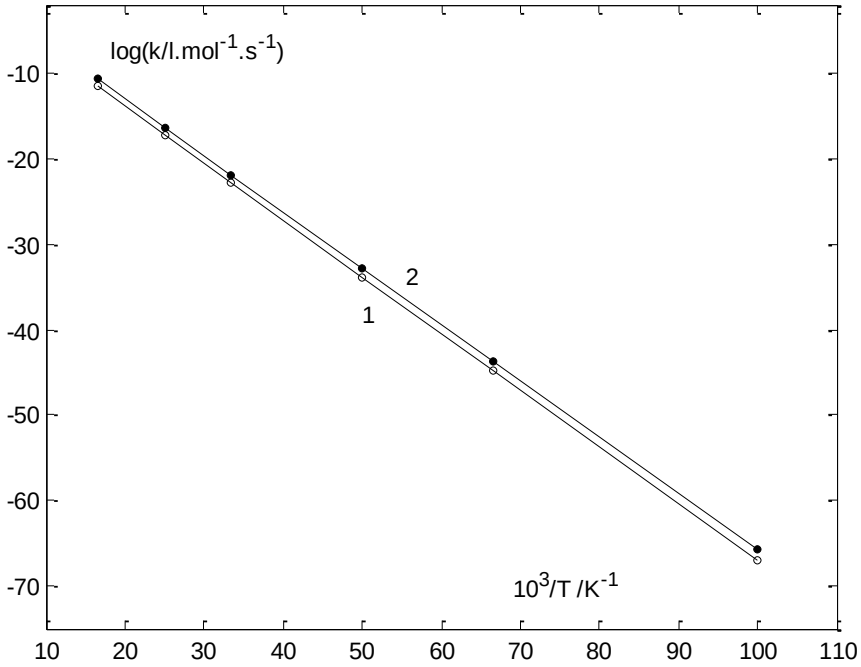

Figure 4. The rate constants *k* over the interval 80 – 10 K; designations – see Figure 3.

In Figure 5, the temperature dependence of the rate constant *k* (curve 1) is compared with the high-level data of Truhlar and Co. [15] (curve 2) and calculated experimental data presented in the review article by Kerr and Moss [16] (curve 3). This model predicts lower values of the velocity constants: in the range of 2000 – 200 K, the difference from the values given in the article [15] is on average 0.5 logarithmic units and increases to 2 units at 100 K. At the moment, it is not clear whether this discrepancy with the data of [15, 16] is due to possible errors in the calculation method (and calculation level) or a certain inadequacy of the model we use.

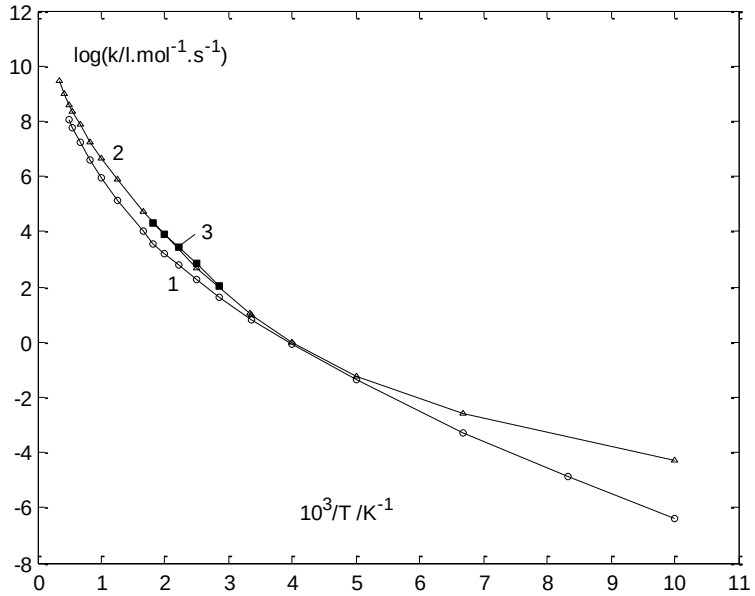

Figure 5. Rate constants: 1 - this study, 2 - theoretical results [15], 3 - evaluated experimental data [16].

4.3 *Energy and frequency characteristics of the reaction. Position Qm.*

Table 5 contains calculated parameters included in the expression for the rate constant k_m (Eq. 5); the distances Q_m and the values of the tunneling frequencies $\nu_{t,m}{}^{0}$, $\nu_{t,m}{}^{i}$ and $\nu_{t,}{}^{m}$ (Eq. 6) are also indicated here.

Consideration of the Table 5 data shows that in the temperature range from 2000 to 10 K, none of the parameters of Eq. 5 remains constant. In accordance with the nature of the observed changes, three temperature ranges can be distinguished: 2000 - 550, 550-80 and 80-10 K. Let's consider them in order.

2000-550 K. This temperature range is characterized by changes in the population of the excited vibrational levels of the potential $V(r|\rho^*,Q)$. At 2000 K the frequency $\nu_{t,m}^{i}$ is ~ 96% of the total frequency ν_t^m; with decreasing temperature, the contribution of excited vibrations gradually decreases and, starting from 550 K, the frequency ν_t^m is completely determined by the frequency of the H-atom transition between zero vibrational levels, $\nu_{t,m}^{0}$. Another aspect of the participation of excited levels in the reaction is a small shift of Q_m to the big side - up to 2.90 Å at 2000 K. With decreasing temperature to 1200 K, Q_m decreases to 2.825 K. The resulting slight increase in the tunneling frequency, $\nu_{t,m}^{0}$, partly compensates for the decrease in $\nu_{t,m}^{i}$. As a consequence, in the temperature range 2000–1200 K, the total transition frequency, $\nu_{t,m}$, decreases relatively weakly. A more significant influence on the value of A_m in this temperature range is exerted by a decrease in the entropy of activation ΔS_m^*. This trend, although to a somewhat lesser extent, persists for the temperature range 1200–600 K.

Table 4. Terms of Eqs. 5a –5c, values of $\nu_{t,m}^{0}$, $\nu_{t,m}^{i}$ and ν_t^m (Eqs. 6a-6c); Q_m

T, K	t, K^{-1}	Q_m, Å	$\nu_{t,m}^{0}$, s^{-1}	$\nu_{t,m}^{i}$, s^{-1}	ν_t^m, s^{-1}	$-\Delta S^*_m$ a)	A_m b)	E_a^m c)	Δh^*_m c)	ΔH_m^* c)
2000	0.5	2.90	7.89(11)	1.93(13)	2.01(13)	17.58	2.90(9)	6.825	7.126	13.950
1800	0.556	2.875	1.53(12)	1.84(13)	1.99(13)	18.02	2.29(9)	7.329	6.438	13.767
1500	0.667	2.85	2.72(12)	1.46(13)	1.73(13)	18.89	1.28(9)	7.833	5.193	13.026
1200	0.833	2.825	4.62(12)	1.08(13)	1.54(13)	19.92	6.80(8)	8.337	3.949	12.286
1000	1.0	2.825	4.62(12)	6.28(12)	1.09(13)	20.65	3.36(8)	8.337	3.154	11.492
800	1.25	2.80	7.48(12)	3.42(12)	1.09(13)	21.64	2.04(8)	8.842	2.340	11.182
600	1.67	2.825	4.62(12)	4.40(11)	5.06(12)	22.53	6.03(7)	8.337	1.663	10.001
550	1.82	2.825	4.62(12)		4.62(12)	22.94	4.16(7)	8.337	1.487	9.824
500	2.0	2.825	4.62(12)		4.62(12)	23.20	3.93(7)	8.337	1.318	9.655
450	2.22	2.875	1.53(12)		1.53(12)	23.27	1.25(7)	7.329	1.250	8.580
400	2.5	2.90	8.22(11)		8.22(11)	23.52	5.97(6)	6.825	1.143	7.967
350	2.86	2.90	8.22(11)		8.22(11)	23.87	4.99(6)	6.825	1.011	7.836
298.15	3.35	2.90	8.22(11)		8.22(11)	24.25	4.12(6)	6.825	0.889	7.714
250	4.0	3.0	4.69(10)		4.69(10)	23.98	2.69(5)	5.242	0.855	6.097
200	5.0	3.025	2.13(10)		2.13(10)	24.22	1.09(5)	4.942	0.782	5.724
150	6.67	3.10	1.73(9)		1.73(9)	24.38	8.12(3)	4.045	0.722	4.767
120	8.33	3.20	4.51(7)		4.51(7)	24.46	206	3.185	0.665	3.850
100	10.0	3.20	4.57(7)		4.57(7)	24.35	217.4	3.185	0.680	3.865
80	12.5	3.30	9.46(5)		9.46(5)	23.88	5.72	2.605	0.654	3.260
60	16.7	3.30	9.46(5)		9.46(5)	23.13	8.34	2.605	0.706	3.311
40	25.0	3.40	1.62(4)		1.62(4)	21.58	0.312	2.254	0.733	2.986
30	33.3	3.40	1.62(4)		1.62(4)	19.46	0.906	2.254	0.806	3.060
20	50.0	3.50	236		236	14.34	0.174	2.118	0.868	2.986
15	66.7	3.50	236		236	13.91	0.215	2.118	0.870	2.989
10	100	3.50	236		236	10.62	1.13	2.118	0.911	3.029

a) e.u. ; b) s^{-1} c) kcal.mol^{-1}

Simultaneously with a decrease in the activation entropy in the range of 2000–550 K, a significant (by ~6 kcal.mol^{-1}) decrease in the enthalpy Δh_m^* occurs. In this case, too, a downward shift in Q_m leads to a weakening of this main effect, this time due to an increase in the energy E_a^m; the resulting decrease in the activation enthalpy ΔH_m^* is ~4 kcal.

Thus, it can be stated that the decrease in the population of excited vibrational levels that occurs in the temperature range of 2000 – 550 K affects the kinetic behavior of the system in two ways: directly, in the form of a decrease in the values of $\nu_{t,m}^{i}$, ΔS_m^*, and Δh_m^*, and indirectly, due to the small decrease in Q_m, an increase in the values of $\nu_{t,m}^{0}$ and E_a^m .

550-80 K. In this temperature range, the value of ΔS_m^* is practically constant, and the changes in Δh_m^* are relatively (compared to changes in E_a^m) small. The competition between the frequency $\nu_{t,m}^{0}$ and the energy E_a^m is

of primary importance. The result of this competition is a gradual shift of the AC towards larger distances Q_m: from 2.825 Å at 550 K to 3.30 Å at 80 K. The reason for these changes is easy to understand if we keep in mind that (1) the tunneling frequency v_t^0, as well as the activation energy E_a, change inversely proportional to the distance Q and (2) the reaction rate constant is proportional to v_t^0 and inversely proportional to E_a, $k \sim v_t^0 \exp(-E_a/RT)$. As a result, the frequency factor shifts Q_m towards lower Q values, and the energy factor - towards higher Q values. With decreasing temperature, the role of the energy factor (due to the factor $t \sim T^{-1}$) increases, leading to a gradual increase in Q_m.

80-10 K. The multiple increase at low temperatures of the factor t determines the dominance of the energy factor. In this regard, the presence of a minimum at Q_m = 3.50 Å on the Q - E_a curve (Figure 2) has a noticeable effect on the course of the temperature dependence of the rate constant. Due to this, with a sufficiently large increase in Q_m (from 3.30 to 3.50 Å), the energy E_a^m decreases only by 0.5 kcal.mol^{-1}. Also, since at low temperatures even a slight increase in the energy of the system in the region Q> 3.50 A sharply decreases the reaction rate, this value, attained at 20 K, turns out to be the limiting one. The shift of Q_m from 3.30 to 3.50 Å causes a significant (by ~3.5 orders of magnitude) decrease in the frequency $v_{t,m}^0$. However, as will be shown below, the influence of this effect on the course of the temperature dependence of the rate constant, due to the dominant role of the energy factor, is insignificant.

4.4 *Analysis of the Arrhenius equation*

4.4.1 *Treatment details; general view of plots for individual terms in Eq. 5*

For the subsequent analysis of the Arrhenius equation, we write down the equations for the rate constant k_m (Eq. 5) in logarithmic form:

$$\log k_m = \log \sigma + \log A_m - (\Delta H_m^*)/2.3RT \quad (11a)$$

$$\log A_m = \log v_t^m + \Delta S_m^*/2.3R \quad (11b)$$

$$-\Delta H_m^*/2.3RT = -E_a^m/2.3RT - \Delta h_m^*/2.3RT \quad (11c)$$

The general view of the term dependences in Eq. 11b on the temperature in the intervals 2000 - 80 and 80 - 10 K are shown in Figures 6 and 7, respectively. Similar dependences for the terms of Eqs. (11c) and (11a) are shown in Figures 8, 9 and 10, 11, respectively. The equations describing the dependencies presented in Figures 6-11 are given in Table 5.

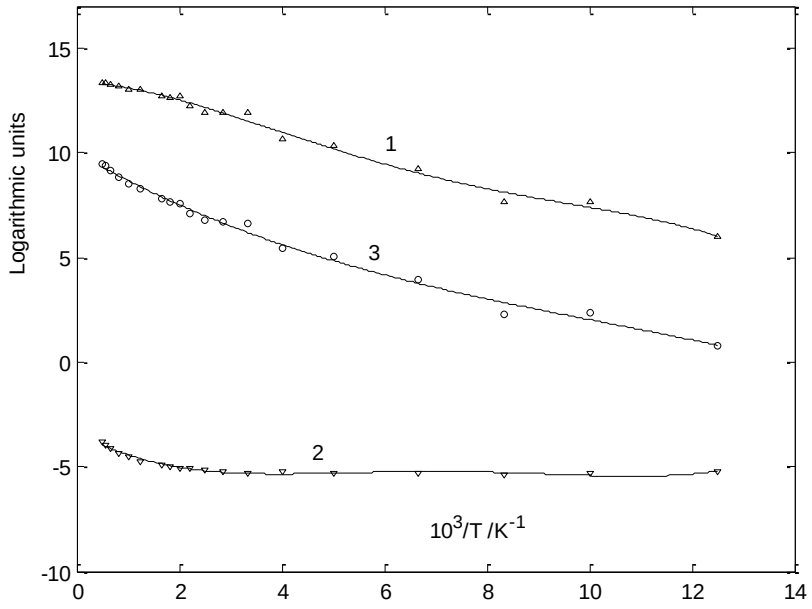

Figure 6. Changes in terms of Eq. (11b) with temperature over the interval 2000 – 80 K: 1 $\log v_t^m$, 2 $\Delta S_m^*/2.3R$, 3 $\log A_m$.

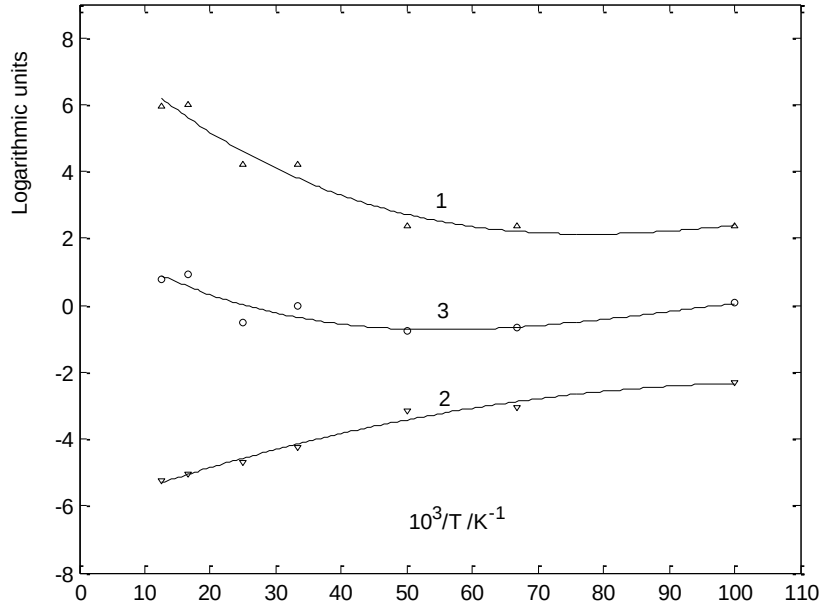

Figure 7. Changes in terms of Eq. (11b) with temperature over the interval 80 – 10 K; designations – see Figure 6.

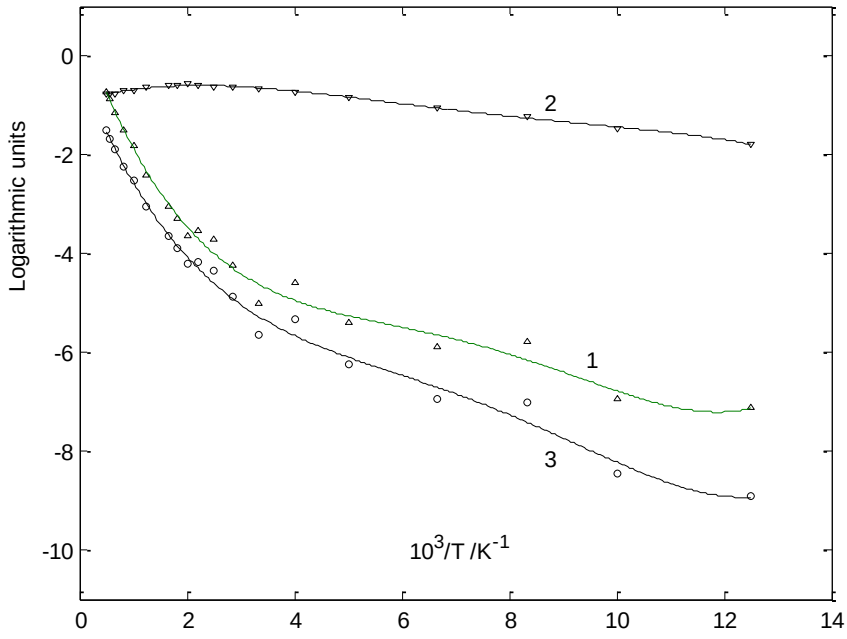

Figure 8. Changes in terms of Eq. (11c) with temperature over the interval 2000 – 80 K: 1 $E_a/2.3RT$, 2 $\Delta h_m^*/2.3RT$, 3 $\Delta H_m^*/2.3RT$

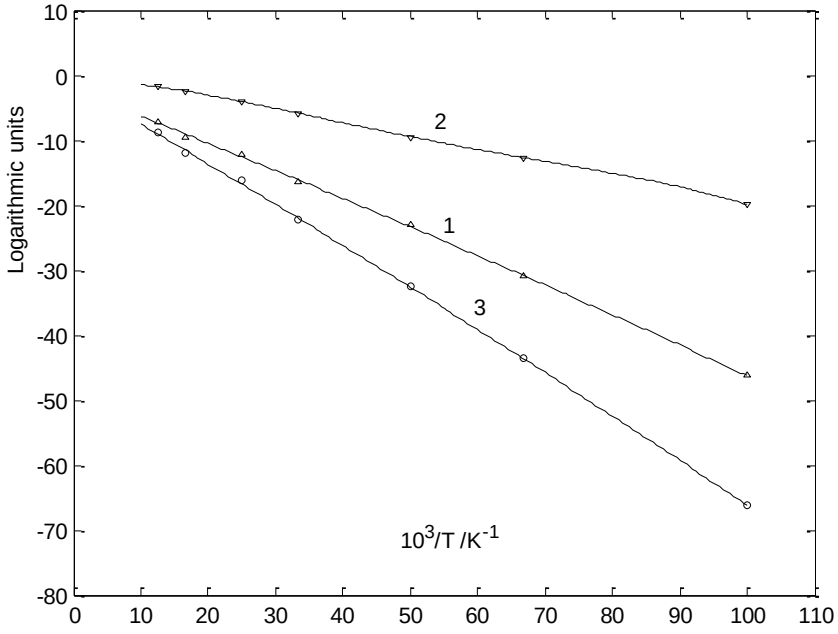

Figure 9. Changes in terms of Eq. (11c) with temperature over the interval 80 – 10 K; designations – see Figure 8.

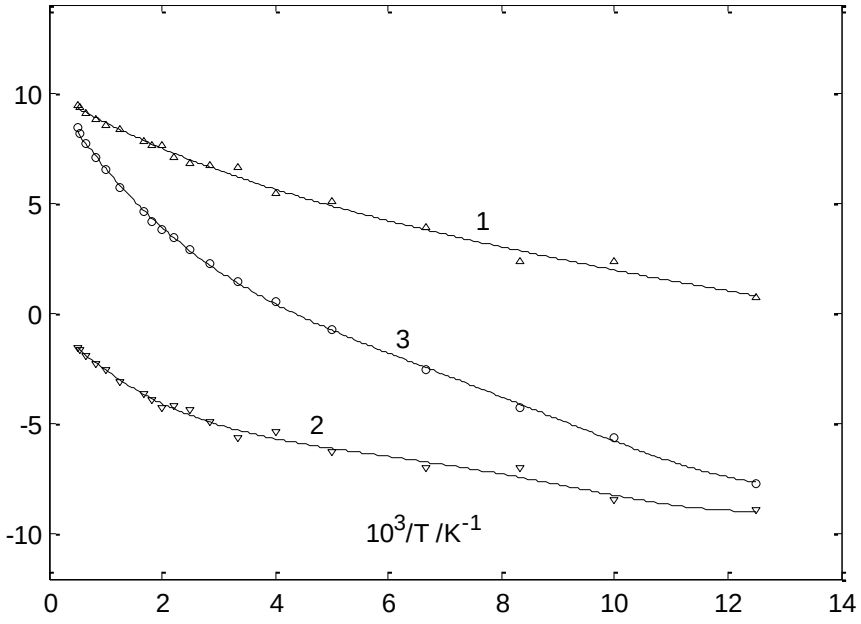

Figure 10. Changes in terms of Eq. (11a) with temperature over the interval 2000 – 80 K: 1 *log* A_m, 2 $\Delta H_m^*/2.3RT$, 3 *log* k_m. Curves 1, 2, and 3 are identical, respectively, to curves: 3 (Figure 6), 3 (Figure 8) and 2 (Figure 4).

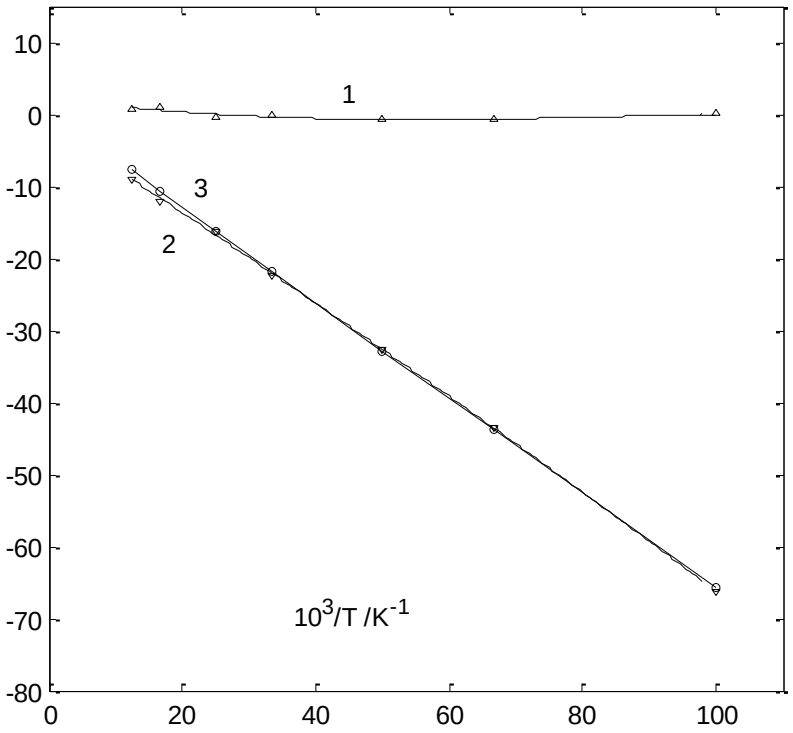

Figure 11. Changes in terms of Eq. (11a) with temperature over the interval 80 – 10 K; designations – see Figure 10. Curves 1, 2, and 3 are identical, respectively, to curves: 3 (Figure 7), 3 (Figure 9) and 2 (Figure 5).

Table 5. The equations of the curves in Figures 6 - 11; $t' = t/2.3R$

Figure[a)]	Curve	2000 – 80 K	80 – 10 K
6, 7	1	$\log v_t^m = -0.421\ t'^4 + 2.48\ t'^3 - 4.43\ t'^2 - 0.501\ t' + 13.39;$	$\log v_t^m = -4.94(-4)\ t'^3 + 0.0382\ t'^2 - 0.868\ t' + 8.28;$
	2	$\Delta S_m^*/2.3R = 0.517\ t'^4 - 3.28\ t'^3 + 7.21\ t'^2 - 6.44\ t' - 3.34;$	$\Delta S_m^*/2.3R = -0.0676\ t'^2 + 0.322\ t' - 6.13;$
	3	$log\ A_m = 0.0967\ t'^4 - 0.807\ t'^3 + 2.79\ t'^2 - 6.94\ t' + 10.06;$	$log\ A_m = 0.013374\ t'^2 - 0.365\ t' + 1.69;$
8, 9	1	$E_a^m/2.3RT = 0.830\ t'^4 - 5.49\ t'^3 + 12.89\ t'^2 - 14.01\ t' + 0.63;$	$E_a^m/2.3RT = - 0.00775\ t'^2 - 1.84\ t' - 2.28;$
	2	$\Delta h^*_m/2.3RT = -0.132\ t'^4 + 0.879\ t'^3 - 2.06\ t'^2 + 1.44\ t' - 0.91;$	$\Delta h^*_m/2.3RT = - 0.0024\ t'^2 - 0.892\ t' + 0.74;$
	3	$\Delta H_m^*/2.3RT = 0.697\ t'^4 - 4.61\ t'^3 + 10.83\ t'^2 - 12.57\ t' - 0.28;$	$\Delta H_m^*/2.3RT - 0.0101\ t'^2 - 2.74\ t' - 1.53;$
10,11	3	$log\ k_m = 0.793\ t'^4 - 5.42\ t'^3 + 13.62\ t'^2 - 19.51\ t' + 10.26$	$log\ k_m = - 3.02\ t' + 0.315;$

a) first number 2000 – 80 K, second 80 – 10 K.

For a more detailed analysis of Eq. 11, we calculated the slope a (coefficient a in the linear equation Eq. 12) and curvature η (doubled value of the coefficient at the first term of the quadratic equation Eq. 13) for limited sections of the corresponding temperature curves. In the first case, the entire temperature range from 2000 to 10 K was divided into eight sections, each of which contained data for four temperatures. In the second case, four intervals were used with data for eight temperatures.

$$y = at + b; \tag{12}$$

$$y^2 = at^2 + bt + c; \tag{13a}$$

$$\eta = 2a. \tag{13b}$$

An analysis of relations 11 using calculated values a and η is given below. A full description of the design parameters for Eqs. (12) and (13) is given in Supplementary Materials (Tables 6S – 11S).

4.4.2 $\log A_m = \log v_t^m + \Delta S_m^*/R$ (Eq. (11b)); Table 6

Slope. In line with the discussion in the previous section, the magnitude of the negative slope of the t - $\log A_m$ plot at high temperatures (2000 - 1200) is determined mainly by changes in the entropy term $\Delta S_m^*/R$; the relatively small (-0.37) value of $a(\log v_t^m)$ reflects the mutual leveling of changes in $\log v_{t,m}^i$ and $\log v_{t,m}^0$. Some predominance of the entropy contribution is also preserved in the interval 1200 – 600 K. In the temperature range of 600 - 80 K, the value of $a(\log A_m)$ is mainly determined by changes in $\log v_{t,m}^0$ as a function of Q_m (an exception is the interval 450 - 298 K, where Q_m is almost constant). A sharp decrease (in absolute value) in the value of $a(v_{t,m}^0)$ at temperatures below 80 K is due to an increase in the interval Δt. For this reason, and also because of the positive value of $a(\Delta S_m^*/R)$, the slope for the t – $\log A_m$ plot in this temperature range is close to zero.

Curvature. The positive curvature ($\eta \sim 1.0$) of the t – $\log A_m$ plot in the range from 2000 to 600 K is determined by the changes in the entropy term, and from 600 to 298 K – in the frequency term. At lower temperatures, the value of $\eta(\log A_m)$, as well as its two components, approaches zero.

Table 6. The values of the slope a (Eq. 12) and curvature η (Eq. 13) for the terms of the equation $\log A_m = \log v_t^m + \Delta S_m^*/2.3R$ (Eq. 11b);

Interval T,K	Δt, K^{-1}	a					Interval T,K	η		
		$\log v_{t,m}^0$	$\log v_{t,m}^i$	$\log v_t^m$	ΔS_m^*/2.3R	$\log A_m$		$\log v_t^m$	ΔS_m^*/2.3R	$\log A_m$
2000-1200	0.333	2.16	-0.78	-0.37	-1.53	-1.90	2000 -600	-0.30	1.29	0.98
1200-600	0.833	0.03	-1.66	-0.54	-0.68	-1.22				
600- 450	0.556	-0.86		-0.86	-0.28	-1.15	600 - 298	0.89	0.09	0.99
450-298	1.13	-0.19		-0.19	-0.19	-0.38				
298-150	3.31	-0.73		-0.73	-0.02	-0.75	298 – 80	0.05	0.01	0.06
150-80	5.83	-0.51		-0.51	0.02	-0.49				
80-30	20.8	-0.10		-0.10	0.05	-0.05	80 - 10	0.02	-0.01	0.00
30-10	66.7	-0.02		-0.02	0.03	0.00				

4.4.3 $-\Delta H_m^*/2.3RT = -E_a^m/2.3RT - \Delta h_m^*/2.3RT$ (Eq. 11c); Table 7

Slope. With decreasing temperature, the slope of the plot t - $\Delta H_m^*/2.3RT$ as a whole consistently changes from -2.1 to -0.7. The decisive contribution to this value is made by the first term of the equation, $E_a^m/2.3RT$. The contribution of the term $\Delta h_m^*/2.3RT$ becomes more noticeable only at low temperatures. Note that for terms of Eq. 11b the value a is the derivative of the parameter P with respect to the variable t, $a = dP/dt$, then in the case of Eq. 11c the value a, being the derivative of the product $P\,t$, can be approximately described by the equation:

$$a = d/dt(P\,t) \approx -P_{mid} - t_{mid}\, dP/dt \qquad (14)$$

Here $P = -U/2.3R$, where U is equal to E_a^m, Δh_m^* or ΔH_m^*; t_{mid} and P_{mid} are the average values of t and P for the given interval Δt, respectively. The details of calculating the values of a according to Eq. 14 are given in Table. 8. The first term in Eq. 14 defines the slope for a "normal" system obeying the standard (linear) Arrhenius equation, while the second reflects the contribution due to the variation of the parameter P. As a rule, an increase in t is accompanied by a decrease in P (Table 4). With a negative value of dP/dt, the second term in Eq. 14 acquires, in contrast to the first, a plus sign. The influence of the second term explains, in particular, the positive slope $a(\Delta h_m^*)$ in the temperature range 2000–450 K. In all other cases, the first term in Eq. 14 exceeds the second in absolute value, which determines the negative slope a for each of the three terms of Eq. 11c.

Curvature. Like the slope, the curvature of the plot t - $\Delta H_m^*/2.3RT$, is determined mainly by changes in the $E_a^m/2.3RT$ term. A characteristic feature of the plot is the change in the sign of the curvature - from positive in the range of 2000 - 600 K to negative in the range of 600 - 298 K[3]. At lower temperatures, the value of η for all three

[3] A positive (negative) value of η in a given temperature range corresponds to a positive (negative) change in the value of a.

terms approaches zero. On the one hand, this is due to a relatively small change in ΔH_m* in this temperature range (Table 4), and on the other hand, a rapid increase in the interval Δt.

Table 7. The values of the slope a (Eq. 12) and curvature η (Eq. 13) for the terms of the equation: $-\Delta H_m^*/2.3RT = -E_a^m/2.3RT - \Delta h_m^*/2.3RT$ (Eq. 11c)

Interval T,K	Δt, K^{-1}	a			Interval T,K	η		
		$\Delta h_m^*/2.3RT$	$E_a^m/2.3RT$	$\Delta H_m^*/2.3RT$		$\Delta h_m^*/2.3RT$	$E_a^m/2.3RT$	$\Delta H_m^*/2.3RT$
2000-1200	0.333	0.19	-2.30	-2.11	2000 -600	-0.14	0.85	0.72
1200-600	0.833	0.14	-1.84	-1.71				
600- 450	0.556	0.00	-0.98	-0.98	600 - 298	-0.03	-0.57	-0.60
450-298	1.13	-0.04	-1.32	-1.35				
298-150	3.31	-0.12	-0.34	-0.46	298 – 80	0.00	0.01	0.01
150-80	5.83	-0.13	-0.25	-0.38				
80-30	20.8	-0.19	-0.43	-0.62	80 - 10	0.00	0.00	0.00
30-10	66.7	-0.21	-0.45	-0.66				

Table 8. Calculation the slope a for the terms of Eq. 12 according to Eq. 14.

Interval T,K	t_{mid}	E_a^m			Δh_m^*			ΔH_m^*		
		$-P_{mid}$	$-t_{mid}\, dP/dt$	a	$-P_{mid}$	$-t_{mid}\, dP/dt$	a	$-P_{mid}$	$-t_{mid}\, dP/dt$	a
2000-1200	0.639	1.657	0.603	-2.260	1.240	1.323	0.082	2.897	0.719	-2.177
1200-600	1.188	1.850	0.021	-1.870	0.607	0.689	0.083	2.456	0.668	-1.788
600- 450	1.927	1.767	0.729	-1.038	0.312	0.314	0.001	2.079	1.042	-1.047
450-298	2.733	1.519	0.215	-1.304	0.235	-0.191	-0.044	1.754	0.406	-1.348
298-150	4.755	1.150	0.762	-0.388	0.177	-0.053	-0.124	1.328	0.815	-0.513
150-80	9.375	0.711	0.457	-0.255	0.149	-0.020	-0.129	0.860	0.476	-0.383
80-30	21.88	0.531	0.096	-0.435	0.158	0.032	-0.190	0.689	0.064	-0.626
30-10	62.5	0.470	0.022	-0.448	0.189	0.019	-0.208	0.659	0.003	-0.656

4.4.4 $\log k_m = \log \sigma + \log A_m - \Delta H_m^*/2.3RT$ (Eq. 11a); Table 9

Slope. Table 9 data give a visual representation of the relative influence of the pre-exponential and energy terms of Eq. 11a in the form of an Arrhenius plot. It can be seen that in a wide temperature range from 2000 to 80 K, these components make approximately the same contribution to the slope of the plot $t - \log k_m$ (the only exception is the temperature range 450 – 298 K, where, due to the constant distance Q_m, the energy contribution is much higher). As already noted, the temperature range below 80 K is dominated by the energy factor. The value $a(\log A_m) \approx 0$, while the value $a(\Delta H_m^*/2.3RT)$ differs noticeably from zero.

Curvature. Even more than the magnitude of the slope, changes in $\log A_m$ affect the curvature of the Arrhenius plot. Thus, it is this factor that determines the positive curvature of the Arrhenius plot in the temperature range of 600 – 298 K. At lower temperatures, the $t - \log k_m$ plot is close to linear. As already noted, the reason for this is, a rapid increase in the value of Δt, as well as relatively small variations in the value of ΔH_m* in this temperature range.

Table 9. The values of the slope a (Eq. 8) and curvature η (Eq. 9) for the terms of the equation $\log k_m = \log A_m - \Delta H_m^*/2.3RT$ (Eq. 11a)

Interval T,K	Δt, K^{-1}	a			Interval T,K	η		
		$\log A_m$	$-\Delta H_m^*/2.3RT$	$\log k_m$		$\log A_m$	$-\Delta H_m^*/2.3RT$	$\log k_m$

2000-1200	0.333	-1.90	-2.11	-4.01	2000 -600	0.98	0.72	1.70
1200-600	0.833	-1.22	-1.71	-2.92				
600- 450	0.556	-1.15	-0.98	-2.13	600 - 298	0.99	-0.60	0.39
450-298	1.13	-0.38	-1.35	-1.74				
298-150	3.31	-0.75	-0.46	-1.20	298 – 80	0.06	0.01	0.07
150-80	5.83	-0.49	-0.38	-0.87				
80-30	20.8	-0.05	-0.62	-0.68	80 - 10	0.00	0.00	0.00
30-10	66.7	0.00	-0.66	-0.66				

5. Conclusion

In conclusion, we note that the above picture of the rate constant temperature dependence of reaction (1) is very close to that observed for the reaction of methane with a methyl radical [1]. In both cases, the non-equilibrium model predicts for the Arrhenius plot a transition with a temperature decreasing from a curvilinear to a linear form of dependence. The main reason for the positive curvature is the change in the pre-exponent caused by the nature of the variation in the entropy of activation (in this case at 2000-600 K) and the frequency of tunneling (at 600-300 K). The region of lower temperatures is characterized by an increasing influence of the enthalpy factor. The transition to a linear form of the reaction rate constant temperature dependence at 80-10 K is determined by a combination of relatively small variations of enthalpy activation with large intervals of Δt.

Conflict of interest

There is no conflict of interest for this study

Supplementary Materials

Table 1S. Imaginary frequencies, ν_{Im}, of the activated complex.

Q, Å	ν_{Im}, cm^{-1}
2.6	254, 132, 22
2.8	186, 118, 59
3.0	163, 118, 74
3.2	176, 131, 85
3.4	208, 151, 94
3.6	245, 173, 99

Frequency assignment. Model 1 (frequency 1–3): CH_3-H-MeOH in-plane deformation, CH_3-H-MeOH out-of-plane deformation, CH_3 group rock vibration.

Table 2S. Thermal corrections to the enthalpy of the activated complex (at a given distance Q), h^*; standard calculation.

Q, Å	T, K							
	500	600	800	1000	1200	1500	1800	2000
2.6	0.094226	0.099841	0.109416	0.120338	0.132318	0.151782	0.172541	0.186900
2.7	0.094440	0.098262	0.107198	0.117468	0.128792	0.147273	0.167053	0.180763
2.8	0.094741	0.098554	0.107486	0.117740	0.129044	0.147495	0.167250	0.180945
2.9	0.094947	0.098797	0.107728	0.117971	0.1290259	0.147687	0.167420	0.181102

Q, Å								
	120	150	200	250	298	350	400	450
2.6					0.088041	0.089414	0.090882	0.092488
2.7					0.088207	0.089599	0.091080	0.092696
2.8			0.086127	0.087238	0.088424	0.089836	0.091332	0.092959
2.9			0.086266	0.087405	0.088613	0.090042	0.091551	0.093188
3	0.084737	0.085306	0.086360	0.087526				
3.1	0.084742	0.085333	0.086420	0.087610				
3.2	0.084737	0.085351						
3.3	0.084729	0.085362						

Q, Å	10	15	20	30	40	60	80	100
3						0.083788	0.084075	0.084391
3.1						0.083750	0.084048	0.084380
3.2						0.083699	0.084011	0.084358
3.3	0.082968	0.083032	0.083095	0.083223	0.083355	0.083644	0.083971	0.084335
3.4	0.082886	0.082949	0.083013	0.083142	0.083278			
3.5	0.082799	0.082862	0.082926	0.083057	0.083198			
3.6	0.082712	0.082775	0.082840	0.082975	0.083123			

Table 3S. Thermal corrections to the free energy of the activated complex (at a given distance *Q*); standard calculation.

Q, Å	*T*, K							
	500	600	800	1000	1200	1500	1800	2000
2.6	0.032974	0.014600	-0.015216	-0.047613	-0.082312	-0.138190	-0.198117	-0.240667
2.7	0.032649	0.019926	-0.007491	-0.037327	-0.069334	-0.120972	-0.176461	-0.215361
2.8	0.032344	0.019516	-0.008136	-0.038203	-0.070438	-0.122411	-0.178230	-0.217348
2.9	0.031969	0.019013	-0.008888	-0.039203	-0.071682	-0.124018	-0.180194	-0.219548

Q, Å	120	150	200	250	298	350	400	450
2.6					0.056167	0.050513	0.044857	0.039008
2.7					0.056050	0.050345	0.044638	0.038737
2.8			0.066211	0.061105	0.055967	0.050208	0.044446	0.038489
2.9			0.066171	0.061018	0.055829	0.050011	0.044191	0.038174
3	0.073791	0.070990	0.066062	0.060855				
3.1	0.073703	0.070876	0.065896	0.060629				
3.2	0.073590	0.070733						
3.3	0.073462	0.070573						

Q, Å	10	15	20	30	40	60	80	100
3						0.078962	0.077311	0.075584
3.1						0.078907	0.077249	0.075510
3.2						0.078833	0.077165	0.075414
3.3	0.082389	0.082085	0.081760	0.081065	0.080326	0.078750	0.077071	0.075304
3.4	0.082305	0.082000	0.081675	0.080978	0.080236			
3.5	0.082216	0.081911	0.081585	0.080886	0.080141			
3.6	0.082128	0.081822	0.081495	0.080794	0.080045			

Table 4S. Thermal corrections to the enthalpy of the activated complex (at a given distance *Q*), *h** (taking into account imaginary frequencies), and reagents, *h* (a.u.)

Q, Å	500	600	800	1000	1200	1500	1800	2000
2.6	0.098007	0.102786	0.113607	0.125783	0.139022	0.160377	0.183031	0.198654
2.7	0.098374	0.103166	0.113988	0.126149	0.139368	0.160693	0.183319	0.198877
2.8	0.098712	0.103544	0.114377	0.126525	0.139725	0.161023	0.183625	0.199220
2.9	0.098971	0.103782	0.114604	0.126742	0.139926	0.161200	0.183781	0.199362
CH_3OH	0.037058	0.062127	0.067936	0.074596	0.081919	0.093836	0.106562	0.072413
CH_3	0.059619	0.038818	0.042688	0.046949	0.051556	0.058999	0.066926	0.115630
Reagents	0.096677	0.100945	0.110624	0.121545	0.133475	0.152835	0.173488	0.188043

Q, Å	120	150	200	250	298	350	400	450
2.6					0.089963	0.091805	0.093732	0.095802
2.7					0.090254	0.092125	0.094073	0.096157
2.8		0.085923	0.087341	0.088901	0.090530	0.092425	0.094390	0.096488
2.9		0.086034	0.087491	0.089085	0.090738	0.092652	0.094631	0.096739
3	0.085262	0.086081	0.087574	0.089195				
3.1	0.085247	0.086087	0.087611	0.089256				
3.2	0.085203							
3.3	0.085160							

CH_3	0.031344	0.031735	0.032409	0.033112	0.033815	0.034603	0.035392	0.036211
CH_3OH	0.052783	0.053203	0.053935	0.054710	0.055509	0.056440	0.057419	0.058478
Reagents	0.084127	0.084938	0.086344	0.087822	0.089324	0.091043	0.092811	0.094689

Q, Å	10	15	20	30	40	60	80	100
3						0.083888	0.084298	0.084742
3.1						0.083838	0.084257	0.084729
3.2						0.083764	0.084189	0.084673
3.3	0.082920	0.082984	0.083047	0.083175	0.083307	0.083691	0.084126	0.084619
3.4	0.082839	0.082902	0.082966	0.083095	0.083230			
3.5	0.082753	0.082816	0.082880	0.083011	0.083151			
3.6	0.082664	0.082727	0.082791	0.082926	0.083074			
CH_3	0.029946	0.030009	0.030073	0.030199	0.030326	0.030579	0.030833	0.031087
CH_3OH	0.051356	0.051420	0.051483	0.051610	0.051736	0.051990	0.052248	0.052512
Reagents	0.081302	0.081429	0.081556	0.081809	0.082062	0.082569	0.083081	0.083599

Table 5S. Thermal corrections to free energy for the activated complex (at a given distance *Q*), *g** (taking into account imaginary frequencies) and reagents, *g* (a.u).

Q, Å	500	600	800	1000	1200	1500	1800	2000
2.6	0.025759	0.010869	-0.021360	-0.056485	-0.094166	-0.154902	-0.220068	-0.266291
2.7	0.025731	0.010756	-0.021636	-0.056925	-0.094765	-0.155734	-0.221127	-0.266899
2.8	0.025660	0.010426	-0.022208	-0.057734	-0.095811	-0.157127	-0.222862	-0.268860
2.9	0.025377	0.010213	-0.022568	-0.058241	-0.096460	-0.157986	-0.223926	-0.270059
CH_3OH	0.009077	-0.001263	-0.023242	-0.046791	-0.071747	-0.111522	-0.153778	-0.183175
CH_3	-0.004135	-0.012535	-0.030225	-0.048939	-0.068544	-0.099418	-0.131839	-0.154217
Reagents	0.004942	-0.013798	-0.053467	-0.095730	-0.140291	-0.210940	-0.285617	-0.337392

Q, Å	120	150	200	250	298	350	400	450
2.6					0.052949	0.046362	0.039741	0.032868
2.7					0.053064	0.046445	0.039788	0.032879
2.8		0.070272	0.064845	0.059043	0.053147	0.046492	0.039798	0.032850
2.9		0.070310	0.064854	0.059012	0.053072	0.046367	0.039621	0.032619
3	0.073345	0.070272	0.064781	0.058897				
3.1	0.073277	0.070189	0.064664	0.058738				
3.2	0.073216							
3.3	0.073108							
CH_3	0.023949	0.022055	0.018728	0.015227	0.011719	0.007812	0.003931	-0.000050
CH_3OH	0.043543	0.041185	0.037070	0.032765	0.028466	0.023688	0.018943	0.014071
Reagents	0.067492	0.063240	0.055798	0.047992	0.040185	0.031500	0.022874	0.014021

Q, Å	10	15	20	30	40	60	80	100
3						0.078865	0.077130	0.075286
3.1						0.078812	0.077075	0.075226
3.2						0.078748	0.077015	0.075166
3.3	0.082341	0.082037	0.081712	0.081017	0.080278	0.078664	0.076925	0.075069
3.4	0.082258	0.081954	0.081628	0.080931	0.080189			
3.5	0.082170	0.081865	0.081538	0.080840	0.080095			
3.6	0.082080	0.081774	0.081447	0.080745	0.079997			
CH_3	0.029645	0.029481	0.029295	0.028879	0.028419	0.027411	0.026317	0.025159
CH_3OH	0.050905	0.050665	0.050404	0.049837	0.049227	0.047918	0.046521	0.045059
Reagents	0.080550	0.080146	0.079699	0.078716	0.077646	0.075329	0.072838	0.070218

Table 6S. Dependence $lgA_m = lgv_t^m + \Delta S_m^*/R$ (Eq. 11b); characteristics of the linear equation (12).

Interval *T*, K	$log\ v_t^m$				$\Delta S_m^*/2.3R$				$log\ A_m$			
	a	*b*	r^2	sd	*a*	*b*	r^2	sd	*a*	*b*	r^2	sd
2000-1200	-0.37	13.49	0.9867	0.04	-1.53	-3.08	0.9980	0.07	-1.90	10.41	0.9976	0.09
1200-600	-0.54	13.63	0.9583	0.11	-0.68	-3.82	0.9828	0.08	-1.22	9.81	0.9947	0.09
600- 450	-0.86	14.21	0.8505	0.38	-0.28	-4.48	0.9274	0.08	-1.15	9.73	0.9326	0.31
450-298	-0.19	12.51	0.6974	0.14	-0.19	-4.66	0.9984	0.01	-0.38	7.84	0.8833	0.14
298-150	-0.73	14.01	0.9565	0.16	-0.02	-5.22	0.6163	0.01	-0.75	8.80	0.9650	0.14
150-80	-0.51	12.44	0.9584	0.11	0.02	-5.49	0.8494	0.01	-0.49	6.95	0.9539	0.11
80-30	-0.10	7.29	0.9113	0.03	0.05	-5.82	0.9964	0.00	-0.05	1.48	0.7482	0.03
30-10	-0.02	4.21	0.6831	0.02	0.03	-4.82	0.9320	0.01	0.00	-0.61	0.2785	0.01

Table 7S. Dependence $-\Delta H_m^*/2.3RT = -E_a^m/2.3RT - \Delta h_m^*/2.3RT$ (Eq. 11c); characteristics of linear equation 12.

Interval *T*, K	$\Delta h_m^*/2.3RT$				$E_a^m/2.3RT$				$\Delta H_m^*/2.3RT$			
	a	*b*	r^2	sd	*a*	*b*	r^2	sd	*a*	*b*	r^2	sd
2000-1200	0.19	-0.88	0.9781	0.03	-2.30	0.40	0.9998	0.03	-2.11	-0.48	0.9991	0.06
1200-600	0.14	-0.82	0.9763	0.02	-1.84	-0.01	0.9948	0.13	-1.71	-0.83	0.9956	0.11
600- 450	0.00	-0.60	0.0159	0.04	-0.98	-1.50	0.8603	0.41	-0.98	-2.09	0.8836	0.37
450-298	-0.04	-0.53	0.9847	0.05	-1.32	-0.54	0.9908	0.13	-1.35	-1.07	0.9917	0.12
298-150	-0.12	-0.26	0.9989	0.00	-0.34	-3.61	0.8739	0.13	-0.46	-3.87	0.9285	0.13
150-80	-0.13	-0.17	0.9964	0.01	-0.25	-4.13	0.8878	0.09	-0.38	-4.30	0.9387	0.10
80-30	-0.19	0.68	0.9981	0.01	-0.43	-1.90	0.9964	0.03	-0.62	-1.22	0.9973	0.03
30-10	-0.21	1.12	0.9998	0.00	-0.45	-0.99	0.9996	0.01	-0.66	0.13	0.9998	0.01

Table 8S. Dependence $log\ k_m = log\ \sigma + log\ A_m - (\Delta H_m^*)/2.3RT$ (Eq. 11a); characteristics of the linear equation 12.

Interval *T*, K	$log\ k_m$			
	a	*b*	r^2	sd
2000-1200	-4.01	10.22	0.9990	0.12
1200-600	-2.92	9.27	0.9984	0.12
600- 450	-2.13	7.94	0.9964	0.13
450-298	-1.74	7.08	0.9999	0.02
298-150	-1.20	5.23	0.9986	0.04
150-80	-0.87	2.96	0.9988	0.03
80-30	-0.68	0.56	0.9999	0.01
30-10	-0.66	-0.18	1.0	0.00

Table 9S. Dependence $lgA_m = lgv_t^m + \Delta S_m^*/2.3R$ (Eq. 11a); coefficient values in the quadratic equation 13.

Interval *T*, K	lgv_t^m			$\Delta S_m^*/2.3R$			lgA_m		
	a	*b*	*c*	*a*	*b*	*c*	*a*	*b*	*c*
2000 - 600	-0.152	-0.171	13.43	0.644	-2.310	-2.86	0.492	-2.48	10.57
600 - 298	0.448	-2.79	16.22	0.047	-0.438	-4.35	0.495	-2.23	11.87
298 - 80	-0.026	-1.01	14.70	-0.004	0.066	-5.08	0.030	-1.08	9.62
80 - 10	0.001	-0.150	7.82	0.000	0.070	-6.13	0.001	-0.080	1.69

Table 10S Dependence $-\Delta H_m^*/2.3RT = -E_a^m/2.3RT - \Delta h_m^*/2.3RT$ (Eq. 11c); coefficient values in the quadratic equation 13.

Interval *T*, K	$\Delta h_m^*/2.3RT$			$E_a^m/2.3RT$			$\Delta H_m^*/2.3RT$		
	a	*b*	*c*	*a*	*b*	*c*	*a*	*b*	*c*

2000 - 600	-0.068	0.306	-0.925	-0.426	-2.90	0.601	0.358	-2.59	-0.324
600 - 298	-0.014	0.031	-0.606	-0.287	0.377	-3.009	-0.301	0.410	-3.62
298 - 80	-0.003	-0.100	-0.312	0.005	-0.343	-3.670	0.003	-0.442	-3.98
80 - 10	0.000	0.195	0.743	0.000	-0.403	-2.281	0.000	-0.598	-1.54

Table 11S. Dependence $log\ k_m = log\ \sigma + log\ A_m - (\Delta H_m^*)/2.3RT$ (Eq. 11a); coefficient values in the quadratic equation 13.

Interval *T*, K	*a*	*b*	*c*
2000 - 600	0.850	-5.08	10.54
600 - 298	0.194	-2.82	8.55
298 - 80	0.034	-1.52	5.93
80 - 10	0.000	-0.678	0.459

References

[1] Romanskii IA. Study of gas-phase reactions within the modified Marcus model. II. $CH_3OH + CH_3 \rightarrow CH_2OH + CH_4$. *Comp. Theor. Chem.* 2018 August; 1138: 66- 74. https://doi.org/10.1016/j.comptc.2018.04.010.

[2] Marcus RA. On the theory of oxidation-reduction reactions involving electron transfer. II. Applications to data on the rates of isotopic exchange reactions. *J. Chem. Phys.* 1957 April; 26(4):867-871.https://doi.org/10.1063/1.1743423

[3] Marcus RA. Theoretical relations among rate constants, barriers and Broensted slopes of chemical reactions. *J Phys Chem*. 1968 March; 72:891-899. https://doi.org/10.1021/j100849a019.

[4] Romanskii IA. Study of gas-phase reactions within the modified Marcus model. IV.Arrhenius equation for the reaction $CH_4 + CH_3 \rightarrow CH_3 + CH_4$. *Reac. Kin. Mech. Cat.* 2022 October; 135:2401-2423. https://doi.org/10.1007/s11144-022-02245-3.

[5] Levich VG, German ED, Dogonadze RR et al. Theory of homogeneous involving proton transfer. *Electochimica Acta* 1970 February;15: 353-367. https://doi.org/10.1016/0013-4686(70)80027-5.

6. German ED, Kuznetsov AM, Dogonadze RR. Theory of the kinetic isotope effect in proton transfer reactions in a polar medium. *J. Chem. Soc., Faraday Trans. 2*. 1970 Augast; 76:1128-1146. https://doi.org/10.1039/F29807601128.

[7] Kuznetsov AM. A quantum mechanical theory of the proton and electron transfer in weakly polar solvents. *J. Electroanal. Chem.* 1986 February; 204:97-109. https://doi.org/10.1016/0022-0728(86)80511-3.

[8]. Romanskii IA. The activated complex position on the reaction coordinate and the problem of curvature – linearity of the Broensted relation. *Comp. Theor. Chem.* 2018 February; 1127: 52-63. https://doi.org/10.1016/j.comptc.2018.01.019.

[9] Romanskii IA. Intramolecular reorganization. Deprotonation of toluene with the $CH2CN^-$ anion: An analysis in the framework of gas-phase model. *Izvestiya Akad. Nauk. Ser. Khim.* 2008; 9:1808-1815 [*Russ. Chem. Bull. Int. Ed.* 2008 September; 57:1842-1849]. https://doi.org/10.1007/s11172-008-0249-7.

[10] Frisch MJ, Trucks GW, Schlegel HB et al. *Gaussian 03 (Revision C.02)*, Gaussian Inc., Wallingford, CT, 2004.

[11] Brickmann J. Proton Motions in Hydrogen Bond. In: Schuster P, Zandel G, Sandorfy C (eds*) The Hydrogen Bond - Recent Developments in Theory and Experiments*, North-Holland Publishing Co., Amsterdam, 1976: 217–244.

[12] Szczesniak MM, Scheiner S. Effects of external ions on the dynamics of proton transfer across a hydrogen bond. *J. Phys. Chem.* 1985 April; 89:1835-1840. https://doi.org/10.1021/j100248a017.

[13] Romanskii IA. (2018) Study of gas-phase reactions within the modified Marcus model. I.CH4+CH3 → CH3 + CH4. *Comp. Theor. Chem.* 2018 February;1125:142-151. https://doi.org/10.1016/j.comptc.2017.12.005.

[14] Alecu IM, Truhlar DG. Computational study of the reactions of methanol with the ydroperoxyl and methyl radicals. 1. Accurate termochemistry and barrier heights. *J. Phys. Chem. A* 2011 March;115: 2811–2829. https://doi.org/10.1021/jp110024e.

[15] Alecu IM, Truhlar DG. Computational study of the reactions of methanol with the hydroperoxyl and methyl radicals. 2. Accurate thermal rate constants. *J. Phys. Chem. A* 2011 November;115: 14599–14611. https://doi.org/10.1021/jp209029p.

[16] Kerr JA, Moss SJ. *CRC Handbook of Bimolecular and Termolecular Gas Reactions*, vol. 1, Boca Raton, FL, CRC Press, 1981.
[17] Hanggi P, Talkner P, Bercovec M. Reaction rate theory: fifty years after Kramers. *Reviews of Modern Physics*. 1990 April; 62:252-341. https://doi: 10.1103/RevModPhys.62.251.